Stepped-Carrier OFDM-Radar Processing Scheme to Retrieve High-Resolution Range-Velocity Profile at Low Sampling Rate

Benedikt Schweizer, *Student Member, IEEE*, Christina Knill, Daniel Schindler, and Christian Waldschmidt, *Senior Member, IEEE*

***Abstract*— Recent publications show that the potential of using orthogonal frequency division multiplexing waveforms as radar signals. Since the range resolution is proportional to the RF bandwidth, the major obstacle that obstructs the practical use in automotive and other low-cost radars is the requirement to sample the received signal at sampling rates that span the whole RF signal bandwidth requiring ADCs with sampling rates in the order of GHz. This paper presents a method to achieve the high range resolution induced by a large RF bandwidth, but with a much lower baseband bandwidth, consequently requiring a much slower ADC while at the same time delivering a velocity profile for each subcarrier. In addition, the processing scheme induces a range migration compensation, independent of the number of targets. This is achieved with barely increased computational effort. The scheme is verified with simulations and measurements at 77 GHz.**

***Index Terms*— Automotive radar, high range resolution, orthogonal frequency division multiplexing (OFDM), processing scheme, range migration, stepped-carrier, stepped-frequency, velocity compensation.**

I. Introduction

WAVEFORMS based on orthogonal frequency division multiplexing (OFDM) are well established in communication systems [1], where they are a standard for wireless communication due to the robustness to channel fading and multipath propagation and multiuser access.

The employment of a multicarrier system based on orthogonal subcarriers for radar operation was first mentioned in [2] and extended with the application of phase codes on the subcarriers that change after each symbol in [3]. In [4], a processing method based on FFT operations is presented. The simultaneous evaluation of range and Doppler information based on OFDM symbols is shown in [5] and [6], and the exact matched filter receiver (RX) was derived in [7] in context of passive radar using digital broadcast signals. A processing scheme to retrieve a 2-D range-velocity image was introduced in [8] and [9], where a method based on so-called "modulation symbols" is presented that is equivalent to matched filtering in the frequency domain and delivers range and velocity of multiple targets unambiguously.

Compared with traditional radar sensors, using OFDM waveforms offers advantages in the field of angle estimation with multiple independent transmitter (TX) and RX antennas (MIMO) simultaneously as orthogonal signals can be transmitted on different frequencies at the same time, what is a frequency division multiplexing (FDM) realization. This concept was introduced in [10] for a simple stepped-frequency technique transmitting continuous waves on multiple antennas that form an OFDM waveform and improved to a scheme using interleaved subcarriers on each antenna in [11]. More advantages include the absence of range-Doppler coupling as it occurs for linear frequency modulated waveforms [12], relatively short symbols resulting in a large unambiguous range and Doppler and the possibility to do simultaneous communication [13]. However, problems such as the large peak-to-average power ratio (PAPR) making amplification inefficient exist, but were addressed in [14].

A major issue of OFDM radar was identified to be the large baseband bandwidth as the whole RF bandwidth needs to be sampled in an ADC. Furthermore, especially for automotive applications, a large bandwidth is needed as it is inversely proportional to the range resolution. Exemplarily, for a range resolution of 5 cm, a bandwidth of 3 GHz is required. It is foreseeable that such ADCs will not be available for the low-cost segment in the near future.

To overcome this issue, methods to reduce the sampling rate need to be developed. The most intuitive approach is called stepped-carrier or stepped-frequency where narrowband OFDM signals are transmitted at multiple carrier frequencies to generate a large RF bandwidth. The use of multiple carrier frequencies was first mentioned in [15] but with a focus on Doppler processing for a single target, while the steps were intended to counteract jammers in an aerospace scenario. The first employment of a stepped-carrier to increase the range resolution is shown in [16]. To achieve a large RF bandwidth, OFDM signals of small bandwidth are used, and the carrier frequency at which they are transmitted is increased by the signal bandwidth after each M symbols. A mathematical model of the signal and processing scheme is given. The high range resolution profile is achieved by using the kth symbol of each block to cover the whole frequency range. However, the

Manuscript received May 24, 2017; revised August 1, 2017; accepted August 31, 2017. Date of publication September 29, 2017; date of current version March 5, 2018. *(Corresponding author: Benedikt Schweizer.)*

B. Schweizer, C. Knill, and C. Waldschmidt are with the Institute of Microwave Engineering, Ulm University, 89081 Ulm, Germany (e-mail: benedikt.schweizer@uni-ulm.de).

D. Schindler is with Corporate Sector Research and Advance Engineering, Robert Bosch GmbH, 70465 Stuttgart, Germany.

Color versions of one or more of the figures in this paper are available online at http://ieeexplore.ieee.org.

Digital Object Identifier 10.1109/TMTT.2017.2751463

profile is only accurate for very small velocity as the target motion between the combined symbols is not considered and a Doppler evaluation is not given.

A similar approach for aerospace applications was pursued in [17], that gives a closed mathematical description and suggests arranging the carrier frequencies according to a Costas scheme [18] to reduce the Doppler impact. As in [16], the high range resolution is calculated by using frequency samples of different blocks. The only difference is that modulation symbols on the diagonal of the single pulses are used and a bank of Doppler filters is suggested to correct the velocity error.

In [19], a software-defined radio platform for stepped-frequency OFDM is presented. In contrast to the previously mentioned approaches, the carrier frequency is not increased after M symbols but after each single symbol, and a range-velocity evaluation is shown. For the combination of the single symbols to one symbol with a large bandwidth, an overlapping subcarrier is used to adjust the phase progression. However, a detailed mathematical description is not given, and this method suffers from the impact of noise on the correction and requires additional processing steps.

As can be seen, a closed processing method to retrieve a 2-D-range-velocity image with velocity compensation for multiple targets is still an open problem. This paper addresses for the first time the synthesis of a high resolution range-velocity profile out of a stepped OFDM waveform with inherent range migration compensation that is suitable for an arbitrary number of targets as it is necessary for automotive applications.

This paper is organized as follows. Section II introduces the stepped signal model. The phase errors caused by stepping the carrier frequency are analyzed in Section III. Based on that, the processing technique is derived in Section IV and verified by simulations in Section V. A measuring setup is explained and radar measurements are shown in Section VI before this paper is concluded in Section VII.

II. Theoretical Background

The OFDM-radar model presented in [20] serves as a basis for the processing scheme derived in this paper. Looking at one OFDM symbol in frequency domain, it is composed of $\mathcal{N}$ subcarriers, which are separated by the frequency Δf. This yields the bandwidth $\mathcal{W} = (\mathcal{N}-1)\Delta f$. To achieve orthogonality, the time duration of one symbol T_s needs to be the reciprocal of the frequency spacing Δf. All carriers of each OFDM symbol are modulated with distinct QPSK phase codes d_{nb}. The generation of such a symbol is conveniently realized in frequency domain, and an IDFT is applied to get the time domain signal of the OFDM symbol. A cyclic prefix of duration T_{cp} that accounts for the maximum expected time of travel is commonly added to prevent from intersymbol interference. With this, the duration of one symbol increases to $T_{\mathrm{sym}} = T_s + T_{\mathrm{cp}}$. A train of $\mathcal{B}$ OFDM symbols using $\mathcal{N}$ subcarriers results in the OFDM Signal

$$\mathcal{X}(t) = \sum_{b=0}^{\mathcal{B}-1}\sum_{n=0}^{\mathcal{N}-1} d_{nb}\, e^{\,j2\pi n\Delta f t}\ \mathrm{rect}\left(\frac{t-bT_{\mathrm{sym}}}{T_{\mathrm{sym}}}\right) \quad (1)$$

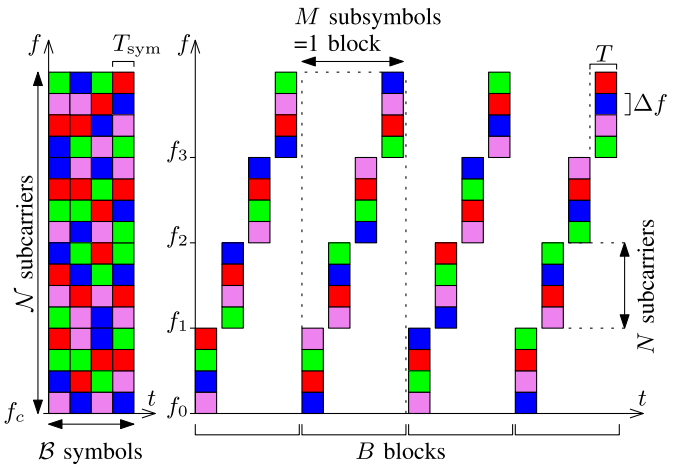

Fig. 1. Structure of OFDM signals in frequency domain. Colors: QPSK codes. Left: standard OFDM. Right: stepping-scheme in RF domain with all parameters.

where d_{nb} denotes the phase code of the nth subcarrier of the bth symbol. Amplitude weighting could be applied to improve signal properties like peak-to-average power ratio [14], but is not considered here.

The signal $\mathcal{X}(t)$ is a wideband baseband signal that occupies the RF channel bandwidth for the whole measurement time $T_{\mathrm{meas}} = \mathcal{B}T_{\mathrm{sym}}$. Thus, the received signal would need to be sampled with the appropriate large sampling rate.

The idea to reduce the baseband bandwidth is to split up each symbol into M subsymbols of which each one has the relatively small bandwidth $W = \mathcal{W}/M$ with $N = \mathcal{N}/M$ subcarriers. To get the full RF bandwidth, which is required for a high range resolution, the subsymbols are upconverted to different carrier frequencies. Those increase by the bandwidth of the baseband signal W after each subsymbol m forming a sawtooth pattern as shown in Fig. 1. The combination of M subsymbols is defined as one block and the stepped-OFDM signal consists of B consecutive blocks. To allow the carrier frequency to settle after a step, a small pause T_{pause} is inserted, leading to the time duration of one subsymbol $T = T_s + T_{\mathrm{cp}} + T_{\mathrm{pause}}$.

With this in mind, the TX baseband signal for stepped OFDM is

$$x(t) = \sum_{b=0}^{B-1}\sum_{m=0}^{M-1}\sum_{n=0}^{N-1} d_{nmb}e^{j2\pi n\Delta f t}\mathrm{rect}\left(\frac{t-bMT-mT}{T}\right) \quad (2)$$

where M represents the number of subsymbols and the phase code d_{nmb} depends on subcarrier, subsymbol, and block. The rectangular term in (2) will be dropped in the further analysis to simplify reading.

To use a larger RF bandwidth, the individual subsymbols in each block are upconverted to the carrier frequency, which is stepped to generate a large RF bandwidth. The stepping is realized in a linear fashion according to

$$f_m = f_c + mN\Delta f \quad (3)$$

as shown in Fig. 1. f_c is the lowest carrier frequency of 77 GHz and f_m is the carrier frequency of the mth subsymbol of each block. The resulting RF waveform

after up-conversion can be formulated as

$$x_{\mathrm{RF}}(t) = \sum_{b=0}^{B-1}\sum_{m=0}^{M-1}\sum_{n=0}^{N-1} d_{nmb} e^{j2\pi(f_m+n\Delta f)t}. \tag{4}$$

A. Channel Model

To describe the radar channel, a simple point scatterer model is used. The received signal is the sum of a delayed and attenuated version of the transmitted signal per target. For L targets, this yields

$$x_{\mathrm{RX}} = \sum_{l=1}^{L} \alpha_l x_{RF}(t-\tau_l). \tag{5}$$

The delay $\tau_l = 2R_{0,l}/c_0$ of the lth target depends on the distance $R_{0,l}$ of the target, and α is a weighting coefficient representing the attenuation. The velocity v_l of a target is defined to be positive for a target approaching the sensor. Including v_l yields

$$R_l(t) = R_{0,l} - v_l t. \tag{6}$$

The delay can consequently be expressed as

$$\tau_l = \frac{2(R_{0,l} - v_l t)}{c_0}. \tag{7}$$

As (4) is only a linear superposition and the processing does not apply nonlinear calculations, it is sufficient to analyze the received radar signal for a single target. The receive signal after down-conversion by f_m for a single target is

$$x_r(t) = \frac{x_{\mathrm{RF}}(t-\tau)}{e^{j2\pi f_m}} = \sum_{b=0}^{B-1}\sum_{m=0}^{M-1}\sum_{n=0}^{N-1} d_{nmb} e^{j2\pi n\Delta f t} \times e^{-j2\pi\frac{2R_0}{c_0}(f_m+n\Delta f)} e^{j2\pi\frac{2v_l}{c_0}(f_m+n\Delta f)}. \tag{8}$$

After sampling with the Nyquist frequency and going to frequency domain by using a DFT, the received modulation symbols of subcarrier n, subsymbol m, and block b can be described as

$$d_{\mathrm{RX},nmb} = d_{nmb} e^{-j2\pi\frac{2R_0}{c_0}(f_m+n\Delta f)} \times e^{j2\pi\frac{2v(m+bM)T}{c_0}(f_m+n\Delta f)}. \tag{9}$$

Thus, there is a phase term depending on the range of a target and a term depending on the velocity in addition to the transmitted modulation symbol. As the transmitted modulation symbols are known, they can be eliminated by an elementwise division resulting in

$$D(n,m,b) = D_{nmb} = \frac{d_{\mathrm{RX},nmb}}{d_{nmb}} = e^{-j2\pi(\frac{2R_0}{c_0}(f_m+n\Delta f))} \times e^{j2\pi(\frac{2v}{c_0}((m+bM)T)(f_m+n\Delta f))}. \tag{10}$$

The next step is to process the received modulation symbols, such that the desired range-velocity profile with high resolution in both dimensions is obtained. Therefore, the M subsymbols of one block need to be combined to one symbol to obtain the desired high-resolution range profile. The traditional approach is to combine the M subsymbols of one block to one vector of length $M \cdot N$, and to apply an IDFT on it to obtain one high-resolution range profile. However, this straightforward approach does not consider any phase errors introduced by the stepping scheme.

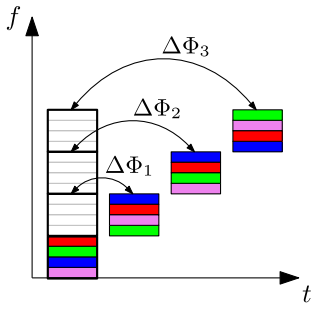

Fig. 2. Phase error $\Delta\Phi_m$ in the stepped-OFDM scheme introduced by sampling the channel at multiple time instances. The Colored blocks represent the time–frequency position of stepped-OFDM signals, whereas the black version shows the corresponding position in a standard OFDM scheme.

III. Range Migration Error

Using subsymbols to sample the full RF bandwidth leads to range migration throughout the subsymbols and, consequently, to a phase error $\Delta\Phi_m$ for each subsymbol compared with the counterpart of a standard OFDM symbol, as shown in Fig. 2.

For a standard OFDM symbol, the phase of the $(mN+n)$th subcarrier at the time instance $t = bMT$ is

$$\mathcal{D}_{nmb} = e^{-j2\pi\frac{2R_0}{c_0}(f_0+n\Delta f)} e^{j2\pi\frac{2vbMT}{c_0}(f_m+n\Delta f)} \tag{11}$$

while for the stepped scenario, the phase of the $(mN+n)$th subcarrier at the time instance $(bM+m)T$, and the phase information is according to (10). Thus, the phase error between a standard OFDM symbol and the stepped-OFDM subsymbol is

$$\Delta\Phi_m = 2\pi\frac{2vmT}{c_0}(f_m+n\Delta f). \tag{12}$$

As can be seen, it depends on the time shift introduced by the stepping-scheme and the target velocity. Thus, the straightforward calculation of the high-resolution range profile would require a unique correction for each velocity what makes this approach that equals a bank of Doppler filters as proposed in [17] computational intensive.

Therefore, a processing technique that does neither depend on single targets nor produce a mathematical overhead but still delivers a 2-D range-velocity profile with the full range resolution is required. Furthermore, a calibration based on an overlapping subcarrier should be avoided as it is only approximative, and the calibration error sums up for every next subsymbol.

IV. Processing Scheme

If the phase error $\Delta\Phi_m$ is compared with the definition of a DFT

$$\mathrm{DFT}[D_{nmb}] = \sum_{b=0}^{B-1} D_{nmb} e^{-j2\pi kbT}, \quad k \in [0, N-1] \tag{13}$$

it is noticeable that the phase error is similar to the exponential term of the DFT. Applying it on the modulation symbols

in time direction delivers a velocity profile $V_{nm}[k]$ with its maximum value for the index k, for which the exponential Doppler term is the complex conjugate of the DFT term, such that the multiplication of both is 1 for each addend

$$e^{j2\pi\left(\frac{2v(m+bM)T}{c_0}(f_m+n\Delta f)\right)}e^{-j2\pi kbT}=1,\quad b\in[0,B-1] \tag{14}$$

resulting in a peak for

$$k=\frac{2v}{c_0}\frac{m+bM}{b}BT \tag{15}$$

where k represents the discretized velocity.

This method corresponds to rearranging the modulation symbols of the stepped-OFDM pattern to a standard $\mathcal{N}\times B$ OFDM pattern, treating the subsymbols as if all of them were transmitted at the time instance of the first subsymbol. As can be seen, the index of the resulting matrix that shows a peak for the velocity v differs depending on the step and also on the summation variable of the DFT. Thus, the velocity profile does not show a sharp peak but is spread over a number of velocity cells. Furthermore, the remaining phase error introduced by the range migration would destroy the range profile calculated from the velocity profile. This is what is expected since the normal DFT would deliver a correct velocity profile for the series of all subsymbols at one carrier, but it still includes the phase shift introduced by the stepping scheme, so the velocity profiles of different carrier frequencies do not fit together.

The solution is to use a modified DFT of the form

$$V_{nm}[k]=\sum_{b=0}^{B-1}D_{nmb}e^{-j2\pi\frac{k(m+bM)}{MB}},\quad k\in[0,N-1] \tag{16}$$

that accounts for the position of the single subsymbols in a $\mathcal{N}\times M\cdot B$ matrix, thus considering the time and frequency shifts as they are constructed by stepping the carrier frequency.

Applying the modified DFT on the modulation symbols yields the condition

$$e^{j2\pi\left(\frac{2v(m+bM)T}{c_0}(f_m+n\Delta f)\right)}e^{-j2\pi\frac{k(m+bM)}{MB}}=1$$
$$b\in[0,B-1],\quad m\in[0,M-1] \tag{17}$$

with the maximum value for the index

$$k=\frac{2v}{c_0}T(f_m+n\Delta f)MB. \tag{18}$$

This is the same velocity profile as it is delivered by a standard OFDM scheme.

Looking at the modified DFT in the alternative form

$$V_{nm}[k]=\sum_{b=0}^{B-1}D_{nmb}e^{-j2\pi k(m+bM)T},\quad k\in[0,N-1] \tag{19}$$

shows, that the modified DFT with k being the Doppler frequency actually considers and corrects the target motion between the samples at one frequency in time direction and also the phase shift that occurs by sampling the range at multiple time instances.

Thus, the desired phase correction can be included into the DFT that delivers the velocity profile. This method does neither increase the computational effort nor the required memory compared with the standard OFDM scheme.

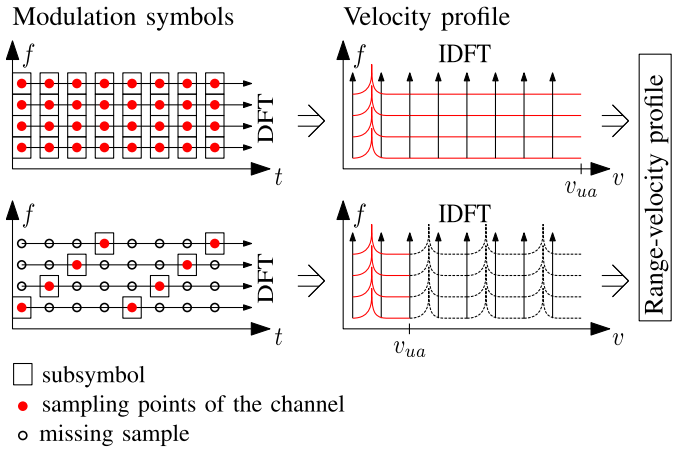

Fig. 3. Visualization of the processing scheme with application of IFFT and FFT on data and zeros for a standard scheme (top) compared with a four-step version (bottom) with the same RF bandwidth. Rectangles: transmitted subsymbols consisting of N subcarriers. Red dots: points in the $t-f$-matrix where the channel was sampled. Black circles: missing points. Arrows: how the DFT is applied using the sampled data and zeros if no data are available.

The practical software realization is to construct a symbol matrix with the dimensions time and frequency that represents the actual time instance and carrier frequency of each subsymbol. The dimensions of the $N\cdot M\times M\cdot B$ matrix are represented by the variables $\eta=n+mN$ and $\mu=m+bM$.

Then, a standard DFT of length $M\cdot B$ is applied in direction of time (μ) to obtain the velocity profile

$$V(\eta,k)=\mathrm{DFT}_\mu\left(\begin{bmatrix}D_{111}&0&D_{112}&0\\D_{211}&0&D_{212}&0\\0&D_{121}&0&D_{122}\\0&D_{221}&0&D_{222}\end{bmatrix}\right). \tag{20}$$

In that way, the modified DFT is reduced to a standard DFT again, but with a velocity range of the standard OFDM scheme. Hence, it has to be limited to the unambiguous velocity of the stepped scheme. The obtained profile is free of phase errors introduced by the stepping scheme but still contains the range information induced by the large RF bandwidth. Finally, an IDFT is applied on the velocity profile in frequency direction (η) to obtain the desired 2-D high-resolution range-velocity profile.

The whole scheme is visualized in Fig. 3 on the basis on subsymbols consisting of N subcarriers in the modulation symbol domain. The rectangles represent transmitted subsymbols, which contain information and sample the channel. Positions where no data are available are marked with a circle. Then, an FFT is applied in direction of time on the symbols. For the standard OFDM scheme, as shown in the top, the DFT uses all sampling points to form a velocity profile for each frequency. In the stepped scheme, desired DFT sampling points are not available. Instead they are replaced by zeros, but the length of the DFT and the starting time instance are the same. This corresponds to undersampling, and thereby reduces the unambiguous velocity by the number of steps, as shown in Fig. 3 (right).

An MIMO-interleaving scheme [11] could be applied on the subcarriers to allow a direction-of-arrival estimation, but this is not the focus of this paper.

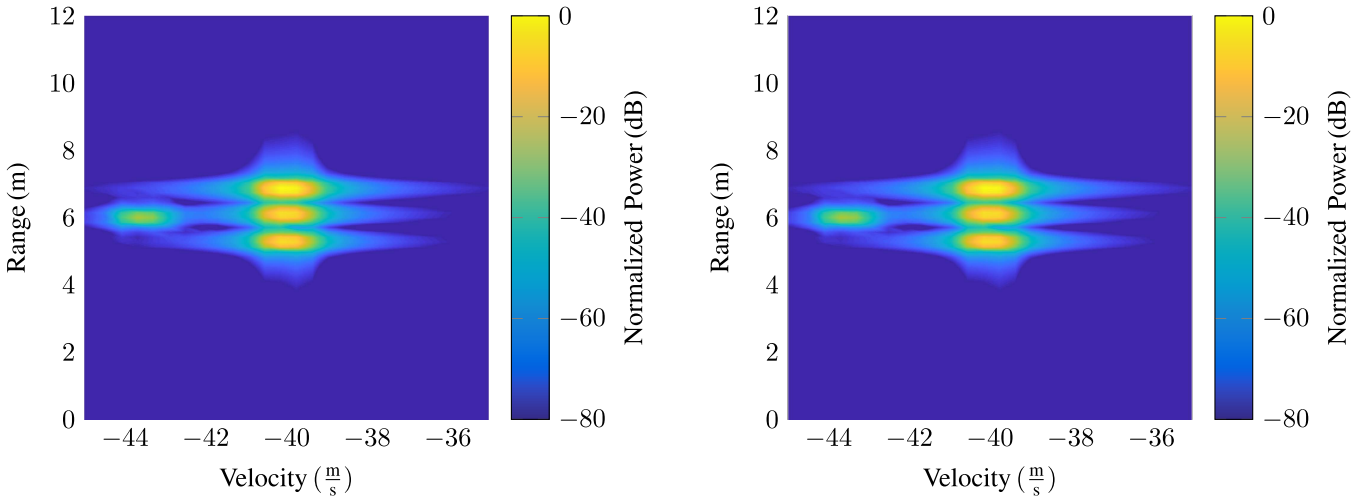

Fig. 4. Simulation results showing suitability for large velocities using targets from Table II. The parameters are according to Table I (one and eight steps). Hann-filtering is applied. Both setups occupy the same RF bandwidth, the same measurement duration, and the same performance. (a) High-resolution reference with 1.024 GHz. (b) Eight steps with 128 MHz each.

A. Performance Evaluation

Compared with a standard OFDM radar, that transmits a waveform spanning the whole RF frequency range for the whole time, the proposed waveform only uses a fraction of the channel bandwidth. But as desired, the range resolution of the stepped scheme equals the conventional one

$$\Delta R = \frac{c_0}{2\mathcal{W}} = \frac{c_0}{2(MN-1)\Delta f}. \tag{21}$$

Due to the steps, each block is M times as long as a standard OFDM symbol. Thus, the Doppler sampling rate is reduced by the factor M. The unambiguously measurable velocity is thereby decreased by M compared with that one of a conventional OFDM radar to

$$v_{\text{ua}} = \pm\frac{c_0}{4f_c T M}. \tag{22}$$

Considering that the OFDM symbols are very short with $T = 2.4\ \mu$s in the measured configuration, this is not a problem by default. If four steps are used, the duration of one block is still below 10 μs corresponding to $v_{\text{ua}} = \pm 101.46$ m/s.

The Doppler resolution

$$\Delta v = \frac{c_0}{2f_c T(M(B-1)+1)} \tag{23}$$

is approximately the same as for a standard OFDM radar, if the measuring time is the same, i.e., the total number of OFDM symbols is fixed ($\mathscr{M} = MB$). The Doppler resolution is not limited by the processing scheme compared with a conventional OFDM radar. Thus, by increasing the number of blocks B, a very high resolution can be achieved.

Depending on the application of the radar, it might be necessary to maximize the unambiguous velocity. This either requires to use fewer subsymbols or to increase the subcarrier spacing Δf, what shortens T_s, thereby increases the unambiguous velocity, and indirectly decreases the unambiguous range

$$R_{\text{ua}} = c_0/(2\Delta f). \tag{24}$$

The time of the cyclic prefix is assumed to be fixed to prevent from intersymbol interference up to the expected maximum range

$$R_{max} = \frac{1}{2}T_{\text{cp}}c_0. \tag{25}$$

In an MIMO configuration with uniform subcarrier interleaving, where the unambiguous range is further decreased, a precise evaluation is required to meet all constraints.

B. Parametrization

To show the practical usability of the proposed scheme, a parametrization is required. Basic constraints are the sampling rate of the ADC and the range resolution, which define the required number of blocks as well as the unambiguous velocity. The subcarrier spacing Δf depends on two conditions, it should be large enough, such that the loss of orthogonality due to the Doppler shift is minimized what requires $\Delta f \geq 10 f_{d,\max}$ as analyzed in [11] and [12] and it must be large enough to obtain the desired unambiguous velocity in combination with the number of subsymbols and the duration of the cyclic prefix.

To achieve a range resolution of $\Delta r \approx 15$ cm, while having a maximum baseband signal bandwidth of approximately 128 MHz available, a setup with $M = 8$ steps is suitable. The subsymbols consist of $N = 256$ subcarriers, spaced by $\Delta f = 500$ kHz. The number of blocks is set to $B = 256$. This leads to the parameters in Table I, which are used for measurements and simulations as well. It should be noted that the total bandwidth is constant with $\mathcal{W} = 1.024$ GHz, as well as the measurement duration. This allows a reliable comparison between standard OFDM (one step) and a stepped-OFDM version with four and eight steps.

TABLE I
RADAR PARAMETERS FOR STEPPED-OFDM RADAR

Subsymbols / Steps	M	1	4	8
Subcarriers	N	2048	512	256
Blocks	B	2048	512	256
RF bandwidth (GHz)	$\mathcal{W}$	1.024		
Baseband bandwidth (GHz)	W	1.024	0.256	0.128
Subcarrier spacing (kHz)	Δf	500		
Duration of cyclic prefix (µs)	T_{cp}	0.4		
Unambiguous range (m)	R_{ua}	300		
Maximum range (m)	$R_{\max}$	60		
Range resolution (m)	ΔR	0.146		
Unambiguous velocity (m/s)	v_{ua}	±405	±101.4	±50.7
Velocity resolution (m/s)	Δv	0.38		

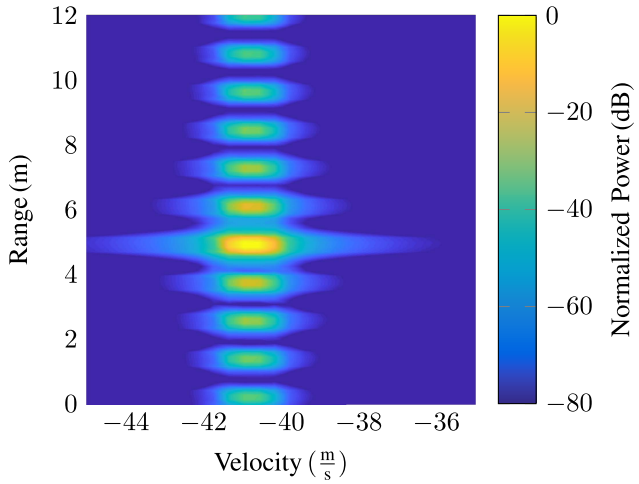

Fig. 5. Violation of unambiguous velocity limit. Simulation results for a stepped-OFDM scheme with eight steps and one target with $R = 5.1$ m and $v = 60$ m/s $> v_{ua}$. Further parameters are $N = 256$, $M = 8$, and $B = 256$. Hann-filtering is applied. Due to the ambiguous velocity, the scheme cannot correct the range migration. Large range sidelobes appear, and the range information is wrong.

C. Signal-to-Noise Ratio

The SNR of an OFDM radar consists of three factors: signal power, noise power, and processing gain. Both, noise power and processing gain are reduced by M compared with a standard OFDM scheme, as the baseband bandwidth and the available modulation symbols are reduced by M to

$$P_{\text{noise}} = kT\frac{\mathcal{B}}{M}F \tag{26}$$

$$G_{\text{processing}} = \frac{\mathcal{N}}{M}B. \tag{27}$$

For the noise power, two limits can be considered: PA limitation and a regulatory approach considering the power spectral density (PSD). In the case of PSD limitations, the overall transmit power can be increased if a larger bandwidth is used. This implies that the TX power of a stepped-OFDM scheme is M times smaller than that of a standard OFDM scheme. The SNR is reduced by M in this case. For PA limitations, it is assumed that the maximum output power of the PA is limited and both schemes exploit the available power. This is particularly true for low-cost on-chip systems.

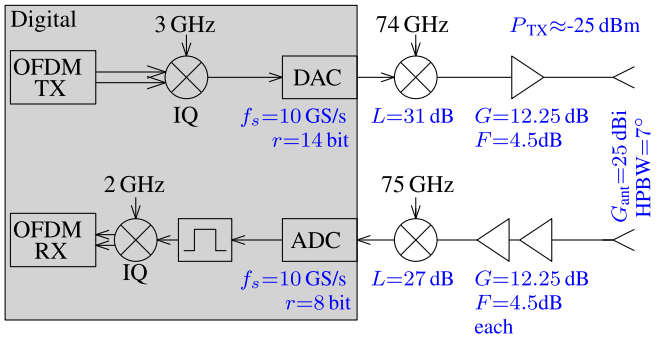

Fig. 6. Schematic of the heterodyne measurement setup.

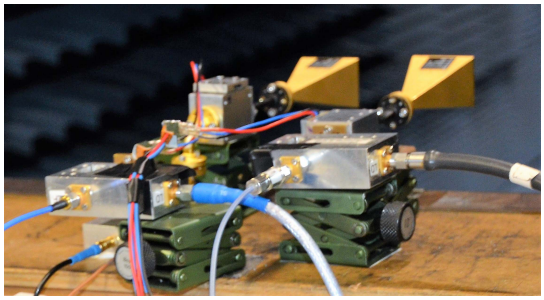

Fig. 7. Photograph of radar setup, including mixer, amplifier, and antennas.

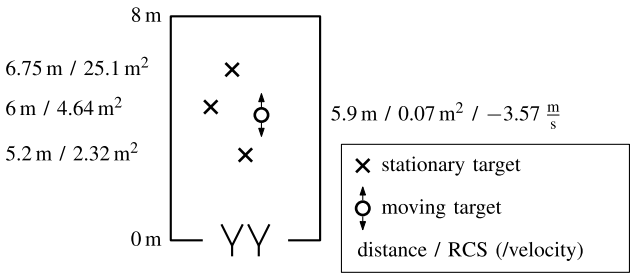

Fig. 8. Scheme of measurement scene consisting of three stationary targets and one moving target.

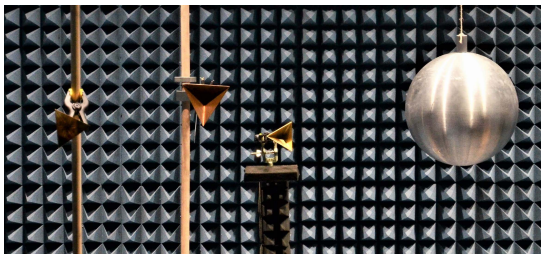

Fig. 9. Photograph of measurement scene with targets according to Fig. 8.

Furthermore, OFDM systems suffer from a PAPR in the order of 8–13 dB [21], causing nonlinear distortions. Therefore, the PA backoff is required to be proportional to the PAPR [22]. Consequently, the RX signal power is the same for both schemes, and the overall achievable SNR does not change.

V. SIMULATION RESULTS

The processing scheme introduced in Section IV is verified with simulations. A simulation model in the equivalent

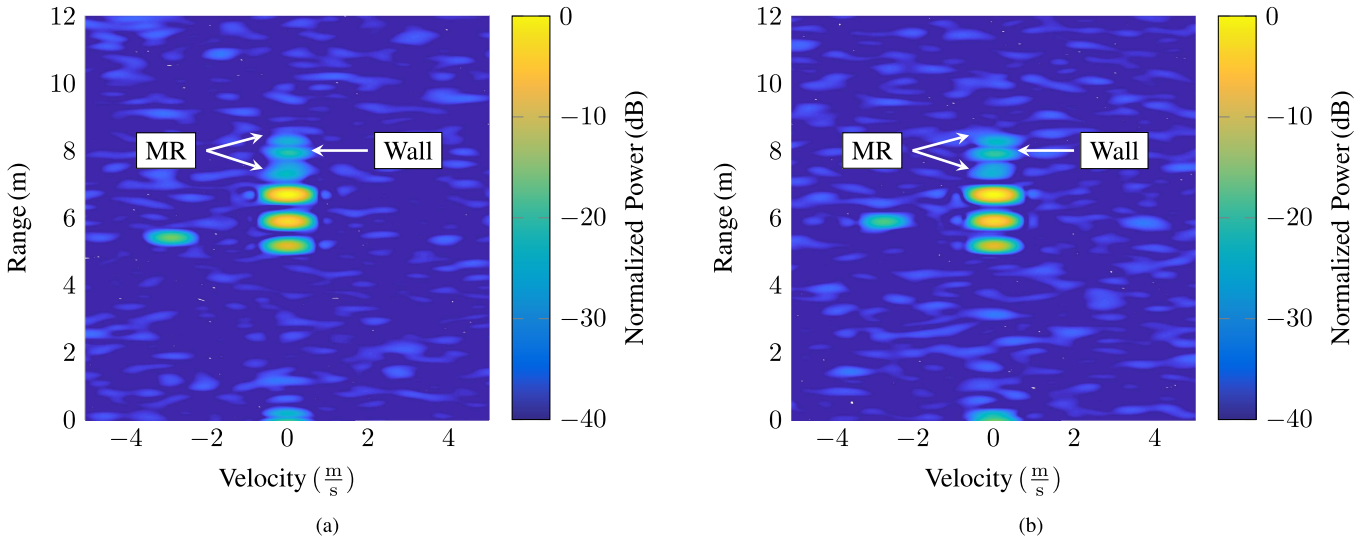

Fig. 10. Measurement results according to the scenario in Fig. 8, zero-padding (factor 8) and Hann-filtering applied. (a) Reference measurement of a standard OFDM setup, consisting of $\mathcal{B} = 2048$ symbols and $\mathcal{N} = 2048$ subcarriers. (b) Measurement for a stepped-OFDM scheme with eight steps of 128 MHz, covering the same RF bandwidth for the same measurement duration. Further parameters are listed in Table I, columns 1 and 8 steps. Both results show almost equal performance. The noise level is barely increased. All targets are at the actual position and clearly separable. Additional targets caused by MRs and the back wall (Wall) are marked.

TABLE II
LIST OF TARGETS USED FOR SIMULATIONS

r (m)	5.2	6	5.9	6.75
v (m/s)	−40	−40	−43.57	−40
RCS (m^2)	2.315	4.64	0.07	25.1

complex baseband is implemented to reduce the required sampling rate to $W = N\Delta f$ while covering the effects of the RF channel by convolving the transmit signal with a frequency-dependent channel impulse response that includes the frequency-dependent Doppler shift and the range information as described in (10). The parameters used for simulation are as listed in Table I, whereby the one-step setup is compared with the eight-step version. The simulated scene consists of four targets as described in Table II. They correspond to the targets used for measurements but with an increased velocity to show the suitability for high velocities. The results shown in Fig. 4 prove that a stepped-OFDM radar with eight steps delivers an almost identical range-velocity plot as a standard OFDM radar. Both are normalized to the strongest target to simplify comparison.

As the unambiguous velocity is $v_{ua} = 50.7$ m/s for eight steps, a target at 5.1 m with a velocity of 60 m/s is shown in Fig. 5. The target folds back into the unambiguous area, ending up at $v = -41.4$ m/s. However, it is noticeable that the processing scheme is not capable of correcting such velocities. This results in large range sidelobes and a wrong range estimation. As a consequence, obeying the unambiguous velocity is critical, when a set of parameters is calculated for a specific scenario.

VI. RADAR MEASUREMENTS

To verify the calculated and simulated results, a 77-GHz OFDM demonstrator based on measurement devices is used. To simplify the setup and to reduce the filtering effort, a heterodyne structure as shown in Fig. 6 is chosen, where the IF stage is realized in the digital domain. Thus, the OFDM baseband signal is generated in software and upconverted to the frequency $f_{c,\mathrm{IF}} = 3$ GHz with a single sideband mixer, such that there is only the upper sideband. The IF signal is fed into an arbitrary waveform generator (AWG), converted into the analog domain and upconverted to the carrier frequency $f_c = 74$ GHz with a diode-based two-sideband subharmonic mixer, amplified and radiated by a standard gain horn antenna. On the receive side, the signal is amplified and downconverted with a carrier frequency of $f_c = 75$ GHz.

In that way both sidebands can be sampled with a 10-GS/s oscilloscope, and the appropriate one can be selected in the digital domain what equals a very sharp bandpass filter. Finally, another IQ mixer is used to convert the signal into the baseband, and it can be evaluated according to the algorithm described in Section IV. The hardware setup as it can be seen in Fig. 7 allows to use a conventional OFDM waveform with a maximum bandwidth of 1 GHz what makes it possible to measure both, a stepped waveform and a reference for comparison and performance evaluation. The measured scene is visualized in Fig. 8 and pictured in Fig. 9 and consists of three stationary targets and a moving target realized with a pendulum. It was conducted in an anechoic chamber. The additional target at 0-m distance is the crosstalk between the TX and the RX. The results are calibrated, such that the targets appear at the actual position as the cables between AWG, radar hardware, and oscilloscope lead to an offset. Further peaks are caused by multiple reflections (MRs) between the actual targets. Also, the back wall of the anechoic chamber is visible at 8 m.

Fig. 10(a) shows the range-velocity plot of the reference measurement with a signal consisting of $\mathcal{N} = 2048$ subcarriers spaced by $\Delta f = 500$ kHz and $\mathcal{B} = 2048$ symbols. This corresponds to a bandwidth of 1.024 GHz and a total

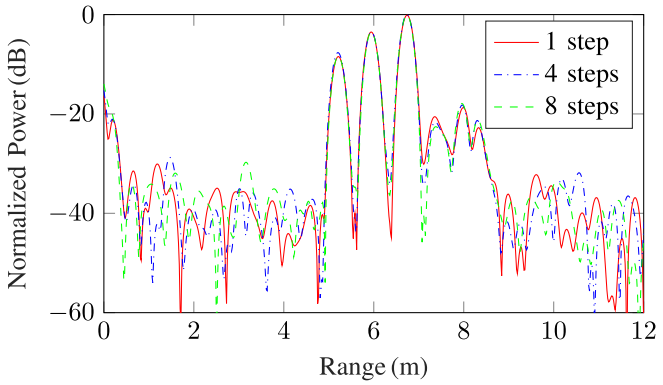

Fig. 11. Measurement results showing the range profile ($v = 0$ m/s) for all configurations of Table I. RF bandwidth and measurement duration are equal for all setups, and Hann-filtering and zero-padding (factor 8) are applied. All curves show the expected targets with almost the same dynamic, despite of a very small deviation at the crosstalk. The noise level is not affected.

measuring time $T_{\text{meas}} = 4.4$ ms. MRs and the back wall are marked in the results. Deviations in the expected target SNR arise from the positions of the individual targets in relation to the narrow beam of the antennas. The moving target does not cause significant MRs as it is mounted far away from the corner reflectors, forming large angles. The actual measurement result for the stepped version with eight steps is shown in Fig. 10(b). It consists of $N = 256$ subcarriers, $M = 8$ subsymbols, and $B = 256$ blocks. Consequently, the measuring time and the total bandwidth are the same as for the high-resolution reference, as well as all parameters that are not mentioned. Comparing both figures reveals that the resolution in range and velocity is nearly the same, all targets are clearly separable. The target distance and velocity corresponds to the actual position and velocity.

To simplify the comparison, a cut at $v = 0$ m/s is shown in Fig. 11 for the reference, and two versions with four and eight steps. All versions cover the same RF bandwidth, but the baseband bandwidth differs. It shows an excellent matching between the reference and the stepped versions for the three actual targets. Also, the noise power stays the same for all configurations. Peak noise positions vary for the different measurements, but the noise is rather constant.

VII. Conclusion

A stepped-carrier OFDM signal is suitable to overcome the limitations of low sampling rate ADCs by modulating baseband symbols of small bandwidth to multiple carrier frequencies forming a sawtooth pattern in the RF channel. The proposed processing scheme based on a modified DFT delivers a range-velocity profile with high resolution in both, range and velocity without increasing the computational effort. Other than previous approaches, it inherently compensates range migration, such that a bank of Doppler filters or a calibration using an overlapping element is unnecessary. The conducted radar measurements show that the performance of a setup with four and eight steps almost equals that one obtained by a reference measurement with the full bandwidth. Only the unambiguous velocity is decreased by the number of steps, what sets an upper limit to the number of steps as to guarantee that the unambiguous velocity is as large as desired. Thereby, also the achievable range resolution is limited by the maximum number of steps in combination with the baseband sampling rate.

References

[1] T. Hwang, C. Yang, G. Wu, S. Li, and G. Y. Li, "OFDM and its wireless applications: A survey," *IEEE Trans. Veh. Technol.*, vol. 58, no. 4, pp. 1673–1694, May 2009.

[2] N. Levanon, "Multifrequency complementary phase-coded radar signal," *Proc. Inst. Elect. Eng.—Radar, Sonar Navigat.*, vol. 147, no. 6, pp. 276–284, Dec. 2000.

[3] N. Levanon and E. Mozeson, "Multicarrier radar signal—Pulse train and CW," *IEEE Trans. Aerosp. Electron. Syst.*, vol. 38, no. 2, pp. 707–720, Apr. 2002.

[4] R. Mohseni, A. Sheikhi, and M. A. M. Shirazi, "A new approach to compress multicarrier phase-coded signals," in *Proc. IEEE Radar Conf.*, May 2008, pp. 1–6.

[5] R. F. Tigrek, W. de Heij, and P. van Genderen, "Solving Doppler ambiguity by Doppler sensitive pulse compression using multi-carrier waveform," in *Proc. Eur. Radar Conf.*, Oct. 2008, pp. 72–75.

[6] R. F. Tigrek, W. de Heij, and P. van Genderen, "Multi-carrier radar waveform schemes for range and Doppler processing," in *Proc. IEEE Radar Conf.*, May 2009, pp. 1–5.

[7] C. R. Berger, B. Demissie, J. Heckenbach, P. Willett, and S. Zhou, "Signal processing for passive radar using OFDM waveforms," *IEEE J. Sel. Topics Signal Process.*, vol. 4, no. 1, pp. 226–238, Feb. 2010.

[8] C. Sturm, E. Pancera, T. Zwick, and W. Wiesbeck, "A novel approach to OFDM radar processing," in *Proc. IEEE Radar Conf.*, May 2009, pp. 1–4.

[9] C. Sturm, M. Braun, T. Zwick, and W. Wiesbeck, "A multiple target Doppler estimation algorithm for OFDM based intelligent radar systems," in *Proc. 7th Eur. Radar Conf.*, Sep. 2010, pp. 73–76.

[10] B. J. Donnet and I. D. Longstaff, "MIMO radar, techniques and opportunities," in *Proc. Eur. Radar Conf.*, Sep. 2006, pp. 112–115.

[11] C. Sturm, Y. L. Sit, M. Braun, and T. Zwick, "Spectrally interleaved multi-carrier signals for radar network applications and multi-input multi-output radar," *Proc. Inst. Elect. Eng.—Radar, Sonar Navigat.*, vol. 7, no. 3, pp. 261–269, Mar. 2013.

[12] G. E. A. F. Franken, H. Nikookar, and P. van Genderen, "Doppler tolerance of OFDM-coded radar signals," in *Proc. Eur. Radar Conf.*, Sep. 2006, pp. 108–111.

[13] D. Garmatyuk, J. Schuerger, Y. T. Morton, K. Binns, M. Durbin, and J. Kimani, "Feasibility study of a multi-carrier dual-use imaging radar and communication system," in *Proc. Eur. Radar Conf.*, Oct. 2007, pp. 194–197.

[14] E. Mozeson and N. Levanon, "Multicarrier radar signals with low peak-to-mean envelope power ratio," *Proc. Inst. Elect. Eng.—Radar, Sonar Navigat.*, vol. 150, no. 2, pp. 71–77, Apr. 2003.

[15] G. Lellouch, P. Tran, R. Pribic, and P. van Genderen, "OFDM waveforms for frequency agility and opportunities for Doppler processing in radar," in *Proc. IEEE Radar Conf.*, May 2008, pp. 1–6.

[16] K. Huo, B. Deng, Y. Liu, W. Jiang, and J. Mao, "The principle of synthesizing HRRP based on a new OFDM phase-coded stepped-frequency radar signal," in *Proc. 10th IEEE Int. Conf. Signal Process.*, Oct. 2010, pp. 1994–1998.

[17] G. Lellouch, A. K. Mishra, and M. Inggs, "Stepped OFDM radar technique to resolve range and Doppler simultaneously," *IEEE Trans. Aerosp. Electron. Syst.*, vol. 51, no. 2, pp. 937–950, Apr. 2015.

[18] J. Costas, "A study of a class of detection waveforms having nearly ideal range—Doppler ambiguity properties," *Proc. IEEE*, vol. 72, no. 8, pp. 996–1009, Aug. 1984.

[19] C. Pfeffer, R. Feger, and A. Stelzer, "A stepped-carrier 77-GHz OFDM MIMO radar system with 4 GHz bandwidth," in *Proc. Eur. Radar Conf. (EuRaD)*, Sep. 2015, pp. 97–100.

[20] C. Sturm and W. Wiesbeck, "Waveform design and signal processing aspects for fusion of wireless communications and radar sensing," *Proc. IEEE*, vol. 99, no. 7, pp. 1236–1259, Jul. 2011.

[21] F. H. Raab *et al.*, "Power amplifiers and transmitters for RF and microwave," *IEEE Trans. Microw. Theory Techn.*, vol. 50, no. 3, pp. 814–826, Mar. 2002.

[22] S. C. Thompson and J. P. Stralka, "Constant envelope OFDM for power-efficient radar and data communications," in *Proc. Int. Waveform Diversity Des. Conf.*, Feb. 2009, pp. 291–295.

Benedikt Schweizer (S'17) received the B.Sc. and M.Sc. degrees in electrical engineering from Ulm University, Ulm, Germany, in 2013 and 2016, respectively, where he is currently pursuing the Ph.D. degree (with a focus on future digital radar systems) at the Institute of Microwave Engineering.

From 2014 to 2015, he was an Intern with the Integrated Circuits Group, Bosch Research and Technology Center North America, Palo Alto, CA, USA.

Christina Knill received the B.Sc. and M.Sc. degrees in electrical engineering from Ulm University, Ulm, Germany, in 2012 and 2015, respectively, where she is currently pursuing the Ph.D. degree at the Institute of Microwave Engineering.

Her current research interests include orthogonal frequency division multiplexing radar signal processing and its application to future adaptive radar sensors for automotive applications.

Daniel Schindler received the B.Sc. and M.Sc. degrees in electrical engineering from the Karlsruhe Institute of Technology, Karlsruhe, Germany, in 2012 and 2015, respectively, and is currently pursuing the Ph.D. degree at Ulm University, Ulm, Germany.

Since 2016, he has been with Corporate Sector Research and Advance Engineering, Robert Bosch GmbH, Stuttgart, Germany. His current research interests include orthogonal frequency division multiplexing-based radar systems.

Christian Waldschmidt (S'01–M'05–SM'13) received the Dipl.Ing. (M.S.E.E.) and Dr.-Ing. (Ph.D.E.E.) degrees from the Karlsruhe Institute of Technology (KIT), Karlsruhe, Germany, in 2001 and 2004, respectively.

From 2001 to 2004, he was a Research Assistant with the Institut fr Hchstfrequenztechnik and Elektronik, KIT. Since 2004, he has been with Robert Bosch GmbH, in the business units Corporate Research and Chassis Systems. He was heading different research and development teams in microwave engineering, RF-sensing, and automotive radar. In 2013, he returned to academia. He was appointed as the Director of the Institute of Microwave Engineering, University Ulm, Germany, where he is currently a Full Professor. He has authored or co-authored over 100 scientific publications and holds over 20 patents. His research interests include radar and RF-sensing, millimeter-wave and submillimeter-wave engineering, antennas and antenna arrays, and RF and array signal processing.

Dr. Waldschmidt is the Vice Chair of the IEEE MTT-27 Technical Committee (wireless enabled automotive and vehicular applications), the Executive Committee Board member of the German MTT/AP Joint Chapter, and a member of the ITG Committee Microwave Engineering. In 2015, he served as the TPC Chair of the IEEE Microwave Theory and Techniques Society International Conference on Microwaves for Intelligent Mobility. He is a Reviewer for multiple IEEE TRANSACTIONS and LETTERS.